

# Deriving daily evapotranspiration from remotely sensed instantaneous evaporative fraction over olive orchard in semi-arid Morocco

J.C.B. Hoedjes, G. Chehbouni, F. Jacob, J. Ezzahar, Gilles Boulet

► **To cite this version:**

J.C.B. Hoedjes, G. Chehbouni, F. Jacob, J. Ezzahar, Gilles Boulet. Deriving daily evapotranspiration from remotely sensed instantaneous evaporative fraction over olive orchard in semi-arid Morocco. Journal of Hydrology, Elsevier, 2008, 254 (1-4), pp.53-64. <ird-00388433>

**HAL Id: ird-00388433**

**<http://hal.ird.fr/ird-00388433>**

Submitted on 28 May 2009

**HAL** is a multi-disciplinary open access archive for the deposit and dissemination of scientific research documents, whether they are published or not. The documents may come from teaching and research institutions in France or abroad, or from public or private research centers.

L'archive ouverte pluridisciplinaire **HAL**, est destinée au dépôt et à la diffusion de documents scientifiques de niveau recherche, publiés ou non, émanant des établissements d'enseignement et de recherche français ou étrangers, des laboratoires publics ou privés.



available at [www.sciencedirect.com](http://www.sciencedirect.com)



journal homepage: [www.elsevier.com/locate/jhydrol](http://www.elsevier.com/locate/jhydrol)



## 2 Deriving daily evapotranspiration from remotely 3 sensed instantaneous evaporative fraction over olive 4 orchard in semi-arid Morocco

5 J.C.B. Hoedjes <sup>a</sup>, A. Chehbouni <sup>a,\*</sup>, F. Jacob <sup>b</sup>, J. Ezzahar <sup>c</sup>, G. Boulet <sup>a</sup>

6 Q3 <sup>a</sup> IRD/CESBIO, UMR: CNES-CNRS-UPS-IRD, 18 Avenue Edouard Belin, 31401 Toulouse Cedex 9, France

7 <sup>b</sup> IRD, UMR LISAH, 2 Place Viala, 34060 Montpellier, France

8 <sup>c</sup> University Cadi-Ayyad, Marrakech, Morocco

Received 7 August 2007; received in revised form 21 January 2008; accepted 24 February 2008

### KEYWORDS

Q4 Evapotranspiration;  
Evaporative fraction;  
Diurnal course;  
Available energy;  
ASTER;  
Semi-arid regions;  
Olive orchard

**Summary** Hydrology and crop water management require daily values of evapotranspiration ET at different time-space scale. Sun synchronous optical remote sensing, which allows for the assessment of ET with high to moderate spatial resolution, provides instantaneous estimates during satellites overpass. Then, usual solutions consist of extrapolating instantaneous to daily values by assuming that evaporative fraction EF is constant throughout the day, providing that daily available energy AE is known. The current study aims at deriving daily ET values from ASTER derived instantaneous estimates, over an olive orchard in a semi-arid region of Moroccan. It has been shown that EF is almost constant under dry conditions, but it depicts a pronounced concave up shape under wet conditions. A new heuristic parameterization is then proposed, which is based on the combination of routine daily meteorological data for characterizing atmospheric dependence, and on optical remote sensing based estimates of instantaneous EF values to take into account the dependence on soil and vegetation conditions. Using the same type of approach, a similar parameterization is next developed for AE. The validation of both approaches shows good performances. The overall method is finally applied to ASTER data. Though performances are reasonably good, their moderate reduction is ascribed to errors on remotely sensed variables. Future works will focus on method portability since its empirical formulation does not account for the direct stomatal response to water availability, as well as on application over different surface and climate conditions.

© 2008 Published by Elsevier B.V.

\* Corresponding author. Tel.: +33 (0)5 61 55 8197; fax: +33 (0)5 61 55 85 00.

E-mail addresses: [joost.hoedjes@cesbio.cnes.fr](mailto:joost.hoedjes@cesbio.cnes.fr) (J.C.B. Hoedjes), [ghani@cesbio.cnes.fr](mailto:ghani@cesbio.cnes.fr) (A. Chehbouni), [frederic.jacob@supagro.inra.fr](mailto:frederic.jacob@supagro.inra.fr) (F. Jacob), [j.ezzahar@ucam.ac.ma](mailto:j.ezzahar@ucam.ac.ma) (J. Ezzahar), [gilles.boulet@cesbio.cnes.fr](mailto:gilles.boulet@cesbio.cnes.fr) (G. Boulet).

## 12 Introduction

13 Estimates of regional evapotranspiration (ET) are of crucial  
14 need for climate studies, weather forecasts, hydrological  
15 surveys, ecological monitoring, and water resource manage-  
16Q1 ment (Van den Hurk et al., 1997; Su, 2000; Bastiaanssen  
17 et al., 2000). Given that distributed hydrological models  
18 can accurately estimate basin scale runoff while poorly  
19 reproducing other hydrological cycle components, interme-  
20 diate processes such as soil moisture and thus ET have to be  
21 well simulated (Chaponnière et al., 2007). Within semiarid  
22 agricultural regions, which hydrological cycle is strongly  
23 influenced by ET through crop water consumption, a precise  
24 ET estimation is of importance for water saving through effi-  
25 cient irrigation practices (Allen, 2000; Ohmura and Wild,  
26 2002; Porporato et al., 2004; Wild et al., 2004). Among  
27 the several research programs designed to develop efficient  
28 irrigation management tools in arid and semi-arid zones, the  
29 SUDMED (Chehbouni et al., in press-a) and IRRIMED ([http://](http://www.irrimed.org)  
30 [www.irrimed.org](http://www.irrimed.org)) projects have taken place in southern  
31 Mediterranean regions, to assess the spatio-temporal vari-  
32 ability of water needs and consumption for irrigated crops  
33 under water limited conditions.

34 Optical satellite remote sensing is a promising technique  
35 for estimating instantaneous and daily ET at global and re-  
36 gional scale, via surface energy budget closure. The meth-  
37 ods proposed in the literature range from simple and  
38 empirical approaches, to complex and data consuming ones  
39 (Glenn et al., 2007). Among the complex methods are Soil  
40 Vegetation Atmosphere Transfer (SVAT) models, which de-  
41 scribe the diurnal course of heat and mass transfers, pro-  
42 vided micrometeorological conditions and water/energy  
43 balance parameters are documented (Braud et al., 1995;  
44 Mahfouf et al., 1995; Olioso et al., 1996; Calvet et al.,  
45 1998; Olioso et al., 2005; Coudert et al., 2006; Gentine  
46 et al., 2007). Among the simple approaches are the simpli-  
47 fied relationship, which links daily ET to midday near sur-  
48 face temperature gradient (Jackson et al., 1977). In the  
49 same vein, the FAO-56 method expresses daily ET using crop  
50 coefficients derived from vegetation indexes, but needs to  
51 be calibrated with ground measurements (Duchemin  
52 et al., 2006; Er-Raki et al., 2007a, Yang et al., 2006). Be-  
53 tween complex and empirical approaches, compromising  
54 solutions are energy balance models. They compute at sat-  
55 ellite overpass instantaneous ET as the residual term of en-  
56 ergy budget, once net radiation, soil heat flux and sensible  
57 heat flux are derived (Bastiaanssen et al., 1998; Norman  
58 et al., 2003; Su, 2002; Caparrini et al., 2003, 2004; French  
59 et al., 2005; Crow and Kustas, 2005; Allen et al., 2007; Cle-  
60 ugh et al., 2007; Mu et al., 2007).

61 Instantaneous values of ET at satellite overpass can be  
62 used as diagnostics for surface status (Chandrapala and  
63 Wimalasuriya, 2003), or as controls for hydrological models  
64 through assimilation schemes (Schuurmans et al., 2003).  
65 However, their interest in terms of water management is  
66 limited, since the latter requires daily values (Bastiaanssen  
67 et al., 2000). Daily ET can be derived from FAO-56 or simpli-  
68 fied relationship, but difficulties raise when extrapolating  
69 outside the environmental conditions considered for cali-  
70 bration. The ET diurnal course can be inferred assimilating  
71 sun synchronous observations into SVAT models, but this is

72 limited by uncertainties when estimating SVAT parameters  
73 and initial variables. The ET diurnal course can also be re-  
74 trieved using geostationary observations, but the kilometric  
75 resolutions severely limit water management at the field  
76 scale. Probably, the most practical solution is estimating  
77 instantaneous values from energy balance models combined  
78 with sun synchronous observations, and next extrapolating  
79 at the daily scale by presuming generic trends for the diur-  
80 nal courses of ET and related variables.

81 Assuming generic trend for the ET diurnal course can  
82 consist of approximating the latter by a sine function, given  
83 it is similar to that of solar irradiance. However, this meth-  
84 od is limited by its empirical character in terms of accuracy  
85 (Zhang and Lemeur, 1995). Another possibility is assuming a  
86 typical shape for Evaporative Fraction (EF) given Available  
87 Energy (AE) is known. The EF is defined as the ratio of ET  
88 to AE, and AE is the difference between net radiation and  
89 soil heat flux. EF is in deed an important indicator of the  
90 surface hydrological history, including wetting and drying  
91 events (Shuttleworth et al., 1989; Nichols and Cuenca,  
92 1993). Thus, it was suggested to assume a constant daytime  
93 EF, to be used with daily AE for deriving daily ET (Sugita and  
94 Brutsaert, 1991; Roerink et al., 2000; Gomez et al., 2005).

95 Assuming a daytime constant EF is not straightforward,  
96 regarding what has been reported from both theoretical  
97 and experimental based investigations (Crago, 1996; Crago  
98 and Brutsaert, 1996). Zhang and Lemeur (1995) observed  
99 EF changes with environmental variables, especially AE  
100 and surface resistance. Suleiman and Crago (2004) reported  
101 that EF increases with vegetation amount, soil moisture and  
102 air dryness. Baldocchi et al. (2004) and Li et al. (2006) re-  
103 ported that stomatal conductance drives EF according to  
104 soil moisture since soil dryness tends to decrease both vari-  
105 ables. During fair weather conditions over fully vegetated  
106 surfaces, Lhomme and Elguero (1999) reported from model  
107 simulation a typical concave-up shape for EF, quite constant  
108 during midday, and mainly driven by changes in soil mois-  
109 ture and solar energy. Thus, assuming a daytime constant  
110 EF equal to the noon value induces underestimations since  
111 this value is the lowest of the day. Finally, Gentine et al.  
112 (2007) showed that EF diurnal course mainly depends on  
113 both evaporative state and vegetation cover. Besides the  
114 EF diurnal course, addressing the daytime AE is a delicate  
115 issue. Empirical approaches have been proposed to derive  
116 it from instantaneous values, mainly approximating AE by  
117 a sine function (Jackson et al., 1983; Bastiaanssen et al.,  
118 2000). Again, the most adequate solution is using geosta-  
119 tionary satellite observations, but the corresponding spatial  
120 resolutions make the use of such data complicated for water  
121 management at field scale.

122 In the same context of the investigations discussed  
123 above, the present study aims at inferring daily ET from  
124 sun synchronous optical remote sensing, with the objective  
125 of improving irrigation water management at the field scale.  
126 The challenge is then considering an irrigated old olive orch-  
127 ard in central Morocco, characterized by a semi-arid cli-  
128 mate, tall trees, and strong soil moisture heterogeneity  
129 due to irrigation practices. This challenge was addressed  
130 in four steps. We first examine the EF diurnal behavior using  
131 Eddy Correlation (EC) measurements, and then quantify  
132 errors on daily ET when assuming EF self-preservation. 132

133 Second, we parameterize the EF diurnal course using a com-  
134 bination of routinely available meteorological data and a  
135 unique "one shot" instantaneous EF estimates. Third, we  
136 parameterize the AE diurnal cycle from ground based mea-  
137 surements of energy balance, also by considering routine  
138 micrometeorological measurements and a single instanta-  
139 neous estimates of AE. Finally, the proposed parameteriza-  
140 tions after being calibrated using ground based data are  
141 applied to ASTER data. These different steps are imple-  
142 mented using data collected during the 2003–2004 period.  
143 Given that ASTER data was only available in 2003, design  
144 and calibration were performed using ground-based 2004  
145 dataset, while validation was performed using the 2003 one.

## 146 Site description and experimental setup

147 The study took place in a semi-arid basin in central Morocco  
148 (the Tensift basin, Fig. 1) within the framework of the SUD-  
149 MED Program (<http://www.irrimed.org/sudmed>). In this  
150 section, site description and experimental setup are briefly  
151 summarized; the reader is referred to *Chehbouni et al.* (in  
152 press-a) for a complete description of both project and site.  
153 The regional climate was characterized by low and irregular  
154 rainfalls with a 240 mm annual average, an evaporative de-  
155 mand of about 1600 mm per year, and a dry atmosphere  
156 with a 56% average humidity. The experiment was carried  
157 out between Day Of Year (DOY) 288 in 2002 and DOY 271  
158 in 2004, at the 275 ha Agdal olive orchard, southeastern of  
159 Marrakech (31°36'N, 07°58'W). The average height of the ol-  
160 ive trees is 6.5 m, the average crown diameter is 6.5 m. The  
161 density of the olive trees at our site is about 225 ha<sup>-1</sup>.  
162 Understorey vegetation consists mainly of short weeds, with  
163 ground cover ranging from almost no (10–20%) cover to al-  
164 most complete (70–80%) cover (*Hoedjes et al., 2007*). The  
165 olive trees are irrigated through level basin flood irrigation.  
166 For this purpose, each tree is surrounded by a small earthen  
167 levy, and water is directed to each tree through a network  
168 of ditches (*Williams et al., 2004*). On average, the irrigation  
169 takes approximately 12 days.

170 The experimental setup collected standard meteorologi-  
171 cal measurements: wind speed and direction (Young Wp200  
172 anemometer); air temperature and humidity (Vaisala  
173 HMP45AC temperature and humidity probe). The instru-  
174 ments were set 9 m above ground (3 m above canopy).

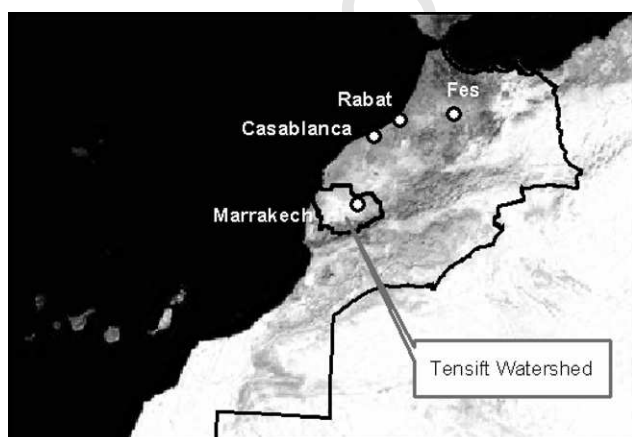


Figure 1 Location of the study area.

The four net radiation components were measured using a  
Kipp and Zonen CNR1 radiometer, set at an 8.5 m height  
to embrace vegetation and soil radiances by ensuring the  
field of view was representative of their respective cover  
fractions. Soil and vegetation brightness temperatures were  
measured using two Apogee IRTS-P. The soil heat flux den-  
sity was measured using heat flux plates (HFT3-L, Campbell  
Scientific Ltd.) at three locations with contrasting amounts  
of radiation reaching the soil. The measurement depth was  
1 cm. The plates were placed: one below the tree, near the  
trunk in order not to be exposed to direct solar radiation;  
one was exposed directly to solar radiation, the last one  
in an intermediate position. An average of these three mea-  
surements was made to obtain a representative value. Soil  
moisture and temperature were recorded at different  
depths within the 0–50 cm horizon, using CS616 water con-  
tent reflectometer and TP107 temperature probes (both  
Campbell Scientific Ltd.), respectively. Measurements were  
sampled at 1 Hz, and 30 min averages were stored on CR10X  
dataloggers (Campbell Scientific Ltd.).

The EC system was installed at a 9.2 m height. During the  
first three months it included a CSAT 3 3D sonic anemometer  
(Campbell scientific Ltd.) and a LICOR-7500 open-path infra-  
red gas analyzer (Campbell Scientific Ltd.). Raw data were  
sampled at a 20 Hz rate, recorded using a CR23X datalogger  
(Campbell scientific Ltd.). After three months, the LICOR-  
7500 was replaced by a KH20 Krypton hygrometer (Campbell  
Scientific Ltd.), and the CR23X was replaced with a CR5000  
datalogger (Campbell Scientific Ltd.). The half-hourly fluxes  
were later calculated off-line using Eddy Covariance pro-  
cessing software 'ECPack', after performing all required  
corrections for planar fit correction, humidity and oxygen  
(KH20), frequency response for slow apparatus, and path  
length integration (*Van Dijk et al., 2004*).

The analysis showed that the sum of latent and sensible  
heat flux measured independently by the EC systems was of-  
ten lower than available energy (AE). The absolute value of  
average closure was about 8% and 9% of available energy  
during the 2003 and 2004 seasons, respectively (*Er-Raki  
et al., 2007b*). This problem could not be explained neither  
by mismatching spatial extents for fluxes and AE measure-  
ments, nor by uncertainties associated with measurements  
of soil heat flux and net radiation (*Twine et al., 2000; Hoed-  
jes et al., 2002; Chehbouni et al., in press-b, 2007c*). Cor-  
rection was then performed using the approach suggested  
by *Twine et al. (2000)*, which assumes the energy balance  
is due to underestimates from EC measurements while the  
corresponding Bowen ratio is correctly estimated. Based  
on this assumption, we re-computed sensible and latent  
heat fluxes by forcing the energy balance using the  
measured AE and Bowen ratio.

ASTER official products (*Abrams and Hook, 2002*) were  
downloaded from the Earth Observing System Data Gateway  
(EDG). Once instrumental effects are removed (*Fujisada,  
1998; Fujisada et al., 1998; Abrams, 2000*), atmospheric  
corrections are performed using radiative transfer codes  
documented for atmospheric status (*Thome et al., 1998*),  
providing surface reflectance's over the solar domain (bands  
1–9) and surface brightness temperatures over the thermal  
domain (bands 10–14). The latter are next used to derive  
surface emissivity and radiometric temperature by applying  
the Temperature Emissivity Separation algorithm (*Gillespie*

237 et al., 1998; Schmugge et al., 1998). Six ASTER images were  
238 collected over the study area, one in 2002 (DOY 311), and 5  
239 in 2003 (DOY 58, 138, 202, 282 and 289). Spatial resolution is  
240 15 m (respectively 30 m) for visible and near infrared  
241 (respectively shortwave) reflectance's, and 90 m for emis-  
242 sivity and radiometric temperature. Higher resolution prod-  
243 ucts were linearly degraded to 90 m, given aggregation  
244 effects from spatial heterogeneities could be considered  
245 as minor over flat semiarid regions (Jacob et al., 2004; Liu  
246 et al., 2006).

247 **Method design, implementation and**  
248 **assessment**

249 The parameterization is designed and assessed using ground  
250 based EC data collected during the 2003–2004 experimental  
251 period. ASTER data were only available in 2003. Therefore,  
252 design and calibration were performed using the 2004 data-  
253 set, whilst validation was performed using the 2003 ground  
254 and ASTER dataset. Furthermore, only daytime observations  
255 from 09:30 to 16:30 UTC are considered, since the most  
256 important latent heat fluxes occur during this period.

257 **EF diurnal course and impact-assessment on ET**  
258 **estimates**

259 In this section we assess the validity of EF self-preservation  
260 using the EC data during dry and wet conditions. It is impor-  
261 tant to mention that dry or wet conditions should normally  
262 be characterized by soil moisture conditions. However,  
263 since we are dealing with the EF which is influenced by both  
264 surface and atmospheric conditions, we preferred instead  
265 to use the Bowen Ratio ( $BR = H/LE$ ) with a threshold value  
266 higher (lower) than 1.5 as indicator of dry (wet) conditions.  
267 Fig. 2a displays the observed diurnal variations of EF as well  
268 as the EF constant value set up to that observed at 11:30  
269 UTC (ASTER time overpass) for 10 cloud free days under  
270 dry conditions, selected between DOY 80 and DOY 221  
271 in 2004. The same curves are presented in Fig. 2b, for a 10-  
272 day cloud free period in 2004 under wet conditions. It can  
273 be seen that that assuming EF self-preservation is valid un-  
274 der dry conditions, since EF is relatively constant despite

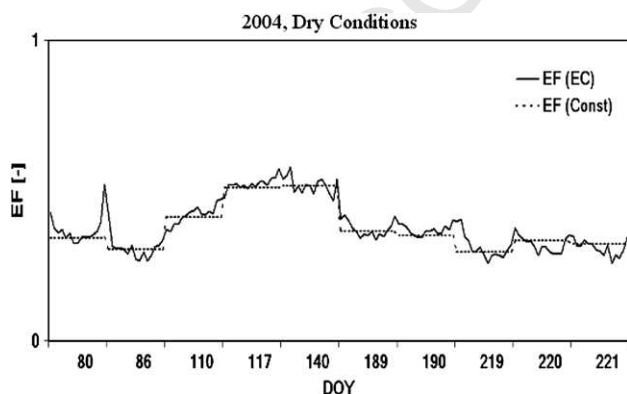


Figure 2a Eddy Covariance (EC) derived evaporative fraction EF (EC) and constant EF (at 11:30) for 10 selected dry and cloud free days within the 2004 selected between DOY 80 and DOY 221.

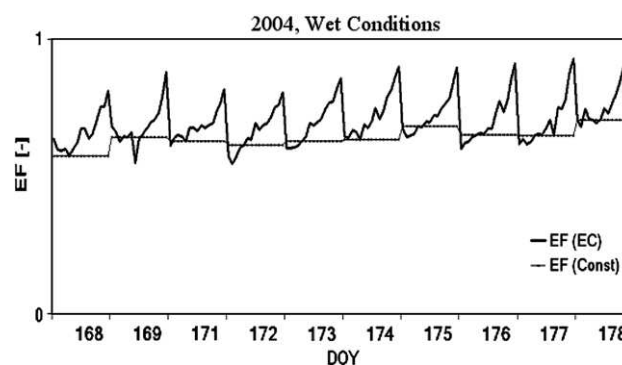


Figure 2b The same as Fig. 2a for 10 wet days following an irrigation event in 2004 (DOY 168–178).

275 observed some daily variation. But this assumption is not valid  
276 under wet conditions, since EF depicts a concave-up  
277 shape with a straight decrease in early morning and a sharp  
278 increase in late afternoon. Thus, assuming EF is constant  
279 and equal to EF @ 11:30 UTC underestimates actual daytime  
280 EF and consequently latent heat flux. These results corroborate  
281 those reported by Lhomme and Elguero (1999), Suleiman and  
282 Crago (2004) and Gentine et al. (2007).

283 Next, we quantify the errors on daytime ET when assum-  
284 ing a constant EF. The ET diurnal course is estimated combin-  
285 ing a daily constant EF and in situ data of AE:

$$286 ET_{EF, const} = EF^{1130} AE = EF^{1130} (R_n - G) \quad (1) \quad 288$$

289 Fig. 3a and b displays comparisons of half hourly ET val-  
290 ues simulated from Eq. (1) against observations for dry and  
291 wet conditions in 2004, respectively. As it might be can be  
292 expected, assuming EF self-preservation appears to be valid  
293 under dry conditions, with an RMSE between observed and  
294 simulated ET of  $14 \text{ W m}^{-2}$  (calibration residual error) and  
295 a Nash–Sutcliffe coefficient of 0.94. Under wet conditions,  
296 however, assuming a constant EF significantly underestimates  
297 ET, with an RMSE between observations and simula-  
298 tions of  $46 \text{ W m}^{-2}$ , and a Nash–Sutcliffe coefficient of

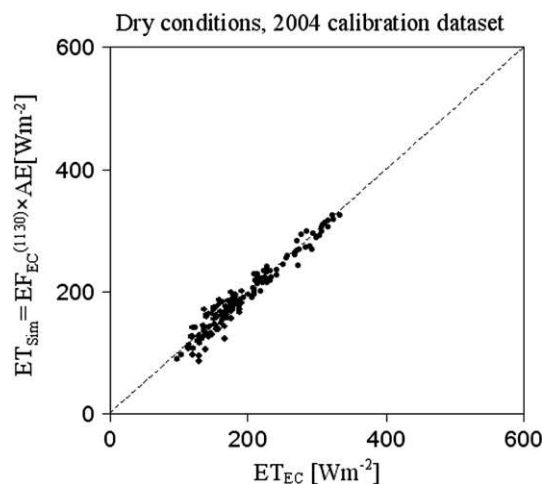
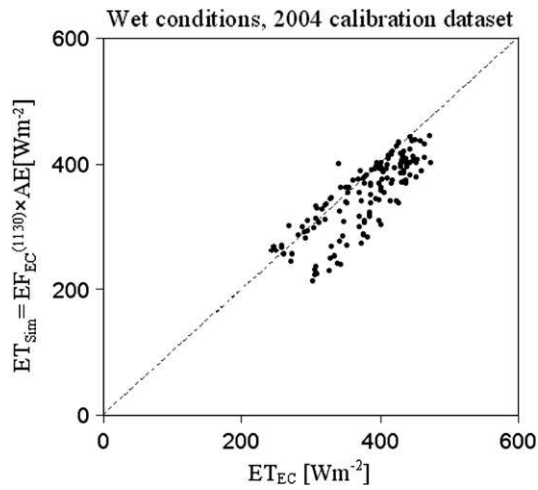


Figure 3a Comparison between eddy covariance latent heat flux ( $ET_{EC}$ ) and latent heat flux calculated using  $EF_{EC}$  at 11:30 as constant during daytime ( $ET_{sim}$ ) during the 10 dry days in 2004.



**Figure 3b** Comparison between eddy covariance latent heat flux ( $ET_{EC}$ ) and latent heat flux calculated using  $EF_{EC}$  at 11:30 as constant during daytime ( $ET_{Sim}$ ) during a 10-day period following an irrigation event in 2004.

299 0.34. Thus, the validity of assuming EF self-preservation de-  
300 pends on soil moisture. It is therefore necessary under wet  
301 condition to account for the diurnal cycle of EF to derive  
302 accurate estimates of daytime ET.

### 303 Parameterizing the EF diurnal cycle

304 An alternative to assuming EF self preservation is proposed  
305 here, through a heuristic approach that parameterizes the  
306 EF diurnal cycle. The constraints are accounting for the EF  
307 daytime relative stability under dry conditions, and ade-  
308 quately reproducing the EF diurnal course during wet  
309 conditions. For operational applications at the irrigation district  
310 scale, the dependence must rely on routinely measured  
311 parameters which remain reasonably constant at such scale,  
312 or on parameters available from remote sensing. Given the  
313 EF diurnal cycle depends on both atmospheric forcing and  
314 surface conditions (Gentine et al., 2007), parameterizing  
315 the diurnal behavior of EF is twofold. First, the diurnal cycles  
316 of atmospheric forcing are considered, since atmospheric  
317 demand is controlled by incoming radiation, relative humid-  
318 ity and, to a lesser extent, wind speed. Second, we account  
319 for land surface heterogeneities potentially available from  
320 remotely sensed thermal data, since control on surface tem-  
321 perature is exerted by vegetation characteristics and most  
322 importantly by soil moisture status.

323 Since an increase in EF mainly results from an increase in  
324 incoming solar radiation and a decrease in atmospheric  
325 humidity (Lhomme and Elguero, 1999; Suleiman and Crago,  
326 2004; Gentine et al., 2007), the first step consists of param-  
327 eterizing the diurnal shape of EF as a function of the main  
328 atmospheric forcing parameters, i.e. incoming solar radi-  
329 ation  $S^{\downarrow}$  and relative humidity RH. The proposed parameter-  
330 ization reads:

$$333 \quad EF_{Sim} = 1.2 - \left(0.4 \frac{S^{\downarrow}}{1000} + 0.5 \frac{RH}{100}\right) \quad (2)$$

Though Eq. (2) provides a good representation of the rela-  
334 tive EF diurnal course, the magnitude and the day-to-day  
335 variation of the EF absolute minimum depend on soil mois-  
336 ture conditions. Therefore, the second step aims at incorpo-  
337 rating, a daily scaling factor in order to produce the actual  
338 day to day variation of EF ( $EF_{Sim}^{ACT}$ ). In order to use effi-  
339 ciently remote sensing data, this scaling factor  $r_{EF}^{1130}$  is ex-  
340 pressed as the ratio of simulated to actual EF when ASTER  
341 overpasses @ 11:30 UTC:

$$342 \quad EF_{Sim}^{ACT} = EF_{Sim} r_{EF}^{1130} \quad (3)$$

343 with

$$344 \quad r_{EF}^{1130} = \frac{EF_{Obs}^{1130}}{EF_{Sim}^{1130}} \quad (4)$$

345 For development purposes,  $EF_{Obs}^{1130}$  is obtained from EC latent  
346 heat observations as well as locally measured AE @ 11:30  
347 UTC, and is written as  $EF_{EC}^{1130}$ . Later on,  $EF_{Obs}^{1130}$  will be derived  
348 from remote sensing data only, using ASTER data to derive  
349 latent heat, and routinely available data to estimate AE;  
350 it will be named  $EF_{ASTER}^{1130}$ .

351 To account for the validity of EF self preservation under  
352 dry conditions which usually corresponds to Bower ratio  
353 values higher than 1.5, the complete EF parameterization  
354 becomes:

$$355 \quad EF_{Sim}^{ACT} = \begin{cases} EF_{Sim} r_{EF}^{1130} & \beta^{1130} \leq 1.5 \\ EF_{Obs}^{1130} & \beta^{1130} > 1.5 \end{cases} \quad \text{for} \quad (5)$$

356 To assess the performance of this proposed parametriza-  
357 tion, we present in Fig. 4 chronicles of measured (EF<sub>EC</sub>)  
358 and simulated (EF<sub>Sim</sub>) EF, for the same 10-day period than  
359 Fig. 2b (2004, wet conditions). Compared to the constant  
360 daytime EF as provided in Fig. 2b, EF<sub>Sim</sub> approximates in a  
361 better way the observed EF diurnal variation (EF<sub>EC</sub>). In or-  
362 der to evaluate the resulting improvement in terms of evap-  
363 oration estimates, latent heat flux is derived from  
364 parameterized EF and in situ observations of AE during the  
365 day:

$$366 \quad ET_{EF,Sim} = EF_{Sim}^{ACT} (R_n - G) \quad (6)$$

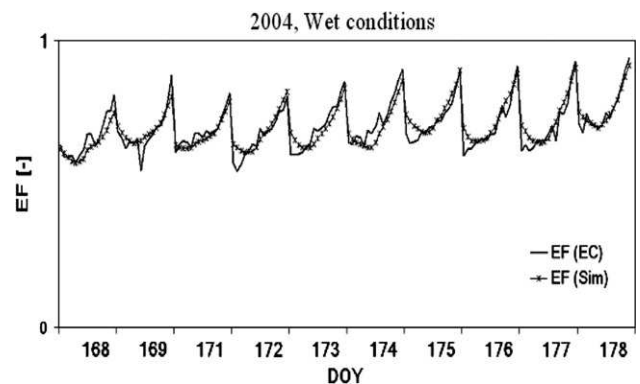


**Figure 4** Comparison between time course of eddy correlation based EF values and those simulated using the parameterization given in Eqs. (2)–(4) for 10 days period under wet conditions in 2004 season.

376 Fig. 5 presents a comparison between measured ET values  
377 and those simulated using Eq. (6) over the 10-day wet period  
378 in 2004. It can be clearly seen that taking into account the  
379 diurnal variation of EF significantly improves ET retrieval.  
380 RMSE between measured and simulated ET values was of  
381  $18 \text{ W m}^{-2}$  and a Nash–Sutcliffe coefficient of 0.9, as com-  
382 pared to  $46 \text{ W m}^{-2}$  and 0.34, respectively when using a con-  
383 stant EF.

384 In order to extend this evaluation with independent data-  
385 set, a 10-day periods (wet conditions) during 2003 were se-  
386 lected. Fig. 6 shows the comparison between  $ET_{EF,Sim}$  and  
387  $ET_{EC}$  including ET estimates when assuming a constant  
388 EF. It is shown that the proposed parameterization for EF  
389 adequately retrieves the observed values of ET compared to  
390 assuming a constant EF during the day. Indeed, RMSE  
391 value is about  $15 \text{ W m}^{-2}$  and the Nash–Sutcliffe coefficient  
392 is 0.90. Finally, the interest of the proposed EF param-  
393 eterization for water balance studies is assessed in terms of

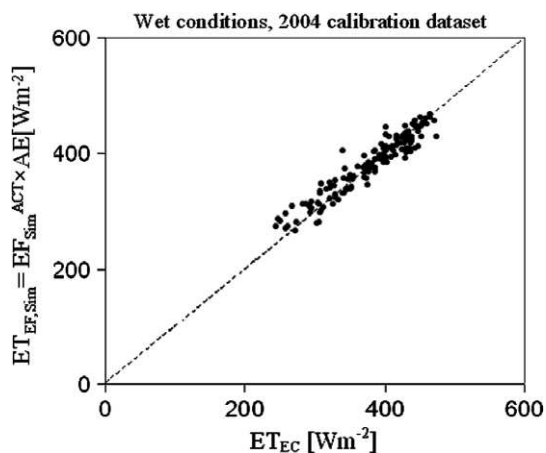


Figure 5 Comparison between measured ET values ( $ET_{EC}$ ) and those simulated using Eq. (6) for the same 10-days period under wet conditions in 2004 season.

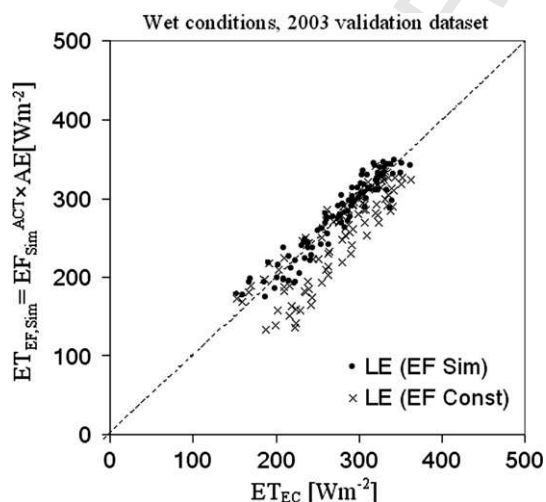


Figure 6 Comparison between  $ET_{EC}$  and  $ET_{Sim}$  during wet conditions in 2003.  $ET_{Sim}$  is calculated both using the proposed parameterization (dots) and, for illustration, using  $EF_{EC}$  at 11:30 as constant daytime value (crosses).

Table 1 Water lost through evapotranspiration during two 10-day wet periods (2004 and 2003, daytime values only); measured, simulated with constant EF and simulated with variable EF

Method	Measured (EC) [mm]	Simulated, Constant EF [mm]	Simulated, Variable EF [mm]
2004	41.3	38.1	41.3
2003	20.9	19.3	21.0

394 water losses through evapotranspiration during the two  
395 wet periods in 2003 and 2004 (Table 1). In both cases, it is  
396 shown using a daytime constant EF for the calculation of  
397 ET underestimated the amount of water lost through evapo-  
398 transpiration by 8%. Conversely, using the proposed EF  
399 parameterization in the calculation of ET reduces the error  
400 on water loss to less than 0.5%.

### 401 Parameterizing the AE diurnal course

402 Implementing Eq. (6) for ET calculation requires the diurnal  
403 course of  $AE = R_n - G$ , which is not routinely available. Var-  
404 ious formulations were proposed for estimating AE at a gi-  
405 ven time of the day (Jackson et al., 1983; Seguin et al.,  
406 1989; Bastiaanssen et al., 2000), usually based on sine func-  
407 tions and thus not accounting for any atmospheric distur-  
408 bance (e.g. Bisht et al., 2005). Another solution is using  
409 instantaneous remote sensing observations when ASTER  
410 overpasses (11:30 UTC), and then extrapolating the AE di-  
411 urnal course from parameterizations based on meteorological  
412 measurements that remain fairly constant at the scale of  
413 the irrigation district. As for the EF parameterization, a heu-  
414 ristic approach is used for the AE diurnal course, by consid-  
415 ering surface net radiation without thermal emission com-  
416 ponent:

$$\left( \frac{(R_n - G)^t}{(R_n - G)_{Obs}^{1130}} \right) = f \left( \frac{R^{*t}}{R^{*1130}} \right) \quad (7)$$

419 where  $R^{*t}$  is a function of solar irradiance ( $S^\downarrow$ ) and atmo-  
420 spheric thermal irradiance ( $L^\downarrow$ ):

$$R^{*t} = (1 - \alpha)S^\downarrow + \varepsilon L^\downarrow \quad (8)$$

421 with  $\alpha$  and  $\varepsilon$  surface albedo and emissivity, respectively.  
422 They are available from remote sensing and are considered  
423 relatively constant throughout the day.  $S^\downarrow$  is available from  
424 meteorological networks or geostationary remote sensors,  
425 and  $L^\downarrow$  can be derived from air temperature and humidity  
426 (Brutsaert, 1982). Assuming albedo is constant throughout  
427 the day can be far from reality (Jacob and Olioso, 2005),  
428 but the validation exercise reported below shows this is  
429 not critical for accurately retrieving the AE diurnal course.  
430 The 2nd order function  $f$  is expressed as:

$$f \left( \frac{R^{*t}}{R^{*1130}} \right) = a_2 \left( \frac{R^{*t}}{R^{*1130}} \right)^2 + a_1 \left( \frac{R^{*t}}{R^{*1130}} \right) + a_0 \quad (9)$$

431 Calibrating Eq. (9) over the EC 2004 dataset provided for  
432 the coefficients:  $a_2 = 0.34285$ ;  $a_1 = 1.15120$ ;  $a_0 = -0.48495$ .  
433 By incorporating Eqs. (8) and (9) into Eq. (7); half hourly AE  
434  
435

441 values are obtained using only diurnal measurements of  $S^{\downarrow}$ ,  
442  $L^{\downarrow}$ , and the single observation  $R_n - G_{Obs}^{130}$  when ASTER over-  
443 passes. Fig. 7a and b displays the comparison between ob-  
444 served and parameterized AE over the two years (2004 for  
445 calibration and 2003 for validation), respectively. For both  
446 cases, it is shown the proposed parameterization is ade-  
447 quate, with RMSE values ranging from  $22 \text{ W m}^{-2}$  for the cal-  
448 ibration dataset to  $30 \text{ W m}^{-2}$  for the validation dataset.

## 449 Application to ASTER data

450 The proposed parameterizations for the AE and EF diurnal  
451 courses rely on standard meteorological data for character-  
452 izing the daytime variations, and on remotely sensed obser-  
453 vations to account for surface heterogeneities induced by  
454 differences in soil moisture and vegetation. Given land sur-  
455 face conditions hardly change throughout the day, and  
456 cloud free meteorological conditions are almost homoge-  
457 neous over the study area, the simulated AE, EF and ET  
458 can be considered as representative. It is thus relevant

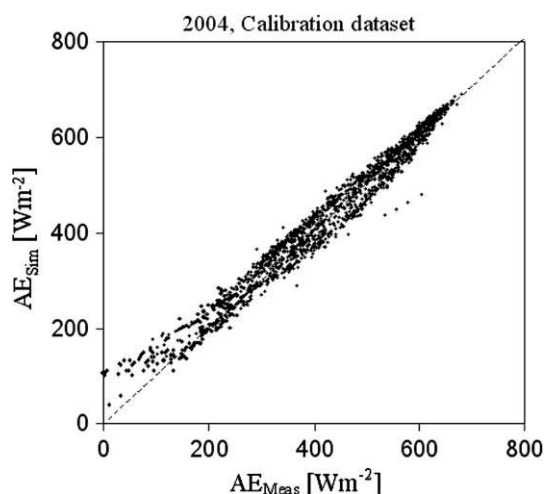


Figure 7a Measured vs. simulated available energy during the whole experimental period in 2004.

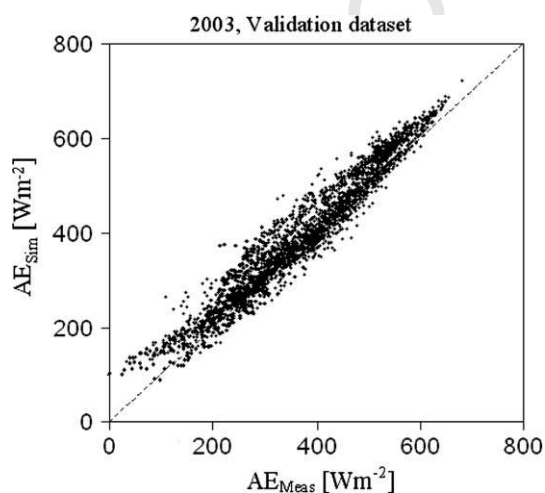


Figure 7b Validation of the AE parameterization for the 2003 experimental season.

459 applying this approach to ASTER observations, which 90 m  
460 spatial resolution for thermal imagery is amongst the finest  
461 possibilities and reduces problems due to mixed pixels  
462 (French et al., 2005). Under unstable conditions, an ASTER  
463 pixel footprint is larger than the source area for a typical  
464 EC system. However, this source area is often located within  
465 adjacent ASTER pixels. A footprint analysis is therefore nec-  
466 essary before any comparison between remote sensing and  
467 in situ observations. To compute the contribution of each  
468 part of the source area (i.e. the footprint of the flux mea-  
469 surement), several approaches have been developed over  
470 the last decades. These range from simple analytical models  
471 (e.g. Schuepp et al., 1990) to complex Lagrangian models  
472 (e.g. Baldocchi, 1997; Rannik et al., 2000) or models based  
473 on large eddy simulations (e.g. Leclerc et al., 1997). As  
474 compared to analytical models, the complex models provide  
475 more realistic footprint simulations over forest canopies,  
476 and they can account for inhomogeneous turbulence. How-  
477 ever, they require significantly larger computational power.  
478 Despite the lack of complexity, Finn et al. (1996) reported  
479 the analytical model proposed by Horst and Weil (1992,  
480 1994) produces very similar results to a Lagrangian stochas-  
481 tic model, and can therefore be considered as a reliable  
482 method. We therefore select this model, which is fully de-  
483 scribed over the same study site in Hoedjes et al., 2007.

## Obtaining fluxes from ASTER observations

484 Calculating land surface net radiation and soil heat flux re-  
485 quires apparent albedo (Jacob and Olioso, 2005), broadband  
486 emissivity over the  $[3-100] \mu\text{m}$  spectral range, and vegeta-  
487 tion cover. Albedo (respectively emissivity) is calculated as  
488 a linear combination of visible and near infrared reflectance  
489 (respectively thermal infrared emissivities), following Jacob  
490 et al. (2002) (respectively Ogawa et al. (2003)) for the  
491 weighting coefficients. Vegetation cover is computed from  
492 Normalized Difference Vegetation Index using the empirical  
493 relationship proposed by Asrar et al. (1984), and following  
494 Weiss et al., 2002 for implementation. Then, net radiation  
495 ( $R_n^{ASTER}$ ) is classically inferred using ASTER derived albedo,  
496 broadband emissivity, and surface radiometric tempera-  
497 ture, along with field observations for solar and thermal  
498 irradiances. The ratio of soil heat flux ( $G^{ASTER}$ ) to net radia-  
499 tion is calculated according to Santanello and Friedl  
500 (2003). Using radiative surface temperature inferred from  
501 ASTER imagery, the semi-empirical model proposed by  
502 Lhomme et al. (1994) is used to obtain sensible heat flux:  
503

$$H^{ASTER} = \rho c_p \left[ \frac{(T_r^{ASTER} - T_a) - c\delta T}{r_a - r_e} \right] \quad (10)$$

504 where  $c_p$  is specific heat of air at constant pressure,  $\rho$  is air  
505 density,  $T_a$  is potential air temperature at reference height  
506 (K) and  $r_a$  is aerodynamic resistance to heat transfer be-  
507 tween the canopy source and the reference height (Brutsa-  
508 ert, 1982). Equivalent resistance  $r_e$  is given by:  
509

$$r_e = \frac{r_{af} r_{as}}{(r_{af} + r_{as})} \quad (11)$$

510 where  $r_{as}$  is aerodynamic resistance between the soil and  
511 the canopy source height (Shuttleworth and Gurney,  
512 1990), and  $r_{af}$  is canopy bulk boundary layer resistance  
513



516 (Choudhury and Monteith, 1988). This one source model is  
517 based on the bulk aerodynamic relationship, but benefits  
518 from a direct use of radiometric surface temperature, in-  
519 stead of aerodynamic surface temperature which is difficult  
520 to estimate (Jacob et al., in press). Furthermore, the tem-  
521 perature difference between the soil and the foliage is taken  
522 into account through the term ( $c\delta T$ ), which is given by:

$$524 \quad \delta T = a(T_r^{\text{ASTER}} - T_a)^m \quad (12)$$

525 and

$$527 \quad c = \left[ \frac{1}{1 + (r_{af}/r_{as})} \right] - f \quad (13)$$

528 Here  $f$  is the fractional vegetation cover,  $a$  and  $m$  are empir-  
529 ical coefficients ( $a = 0.25$  and  $m = 2$ ).

530 Using the footprint model, EC footprint weighted aver-  
531 ages for  $R_n^{\text{ASTER}}$ ,  $G^{\text{ASTER}}$  and  $H^{\text{ASTER}}$  are calculated for each AS-  
532 TER image acquisition. From these average values, the  
533 instantaneous EF, AE and Bowen ratio are estimated on AS-  
534 TER overpass as

$$AE^{\text{ASTER}} = R_n^{\text{ASTER}} - G^{\text{ASTER}} \quad (14)$$

$$EF^{\text{ASTER}} = \frac{R_n^{\text{ASTER}} - G^{\text{ASTER}} - H^{\text{ASTER}}}{R_n^{\text{ASTER}} - G^{\text{ASTER}}} \quad (15)$$

$$536 \quad \beta^{\text{ASTER}} = \frac{H^{\text{ASTER}}}{R_n^{\text{ASTER}} - G^{\text{ASTER}} - H^{\text{ASTER}}} \quad (16)$$

### 537 Application of the methods

538 Fig. 8a and b displays the validation of  $H^{\text{ASTER}}$  against  $H_{\text{EC}}$   
539 and of  $AE^{\text{ASTER}}$  against measured AE, for the 6 ASTER imag-  
540 ery acquisitions. The corresponding RMSE values between  
541 ground based and ASTER based estimates were  $27 \text{ W m}^{-2}$   
542 for  $H$  and  $51 \text{ W m}^{-2}$  for AE. From these estimates, instan-  
543 taneous EF and Bowen ratio are calculated using Eqs. (15) and  
544 (16). A comparison between  $EF^{\text{ASTER}}$  and  $EF_{\text{EC}}$  is shown in  
545 Fig. 9, the corresponding RMSE value being 0.06. Despite  
546 some scatter, results are comparable to those reported in  
547 earlier studies (Crow and Kustas, 2005; Batra et al., 2006;  
548 Wang et al., 2006). From the calculated Bowen ratio values,  
549 it is possible to examine occurrences of wet and dry condi-  
550 tions over the six days of ASTER imagery acquisition. Dry  
551 conditions were observed on one day, with  $\beta^{\text{ASTER}} > 1.5$ .  
552 On two days, wet conditions were due to irrigation events  
553 within one week before ASTER overpasses, with  $\beta^{\text{ASTER}}$  from  
554 0.7 to 0.8. On three days, conditions were intermediate,  
555 with  $\beta^{\text{ASTER}}$  from 1.1 to 1.3.

556 Once inferred, instantaneous  $EF^{\text{ASTER}}$  is used in place of  
557  $EF_{\text{Obs}}^{1130}$  in the parameterization scheme (Eqs. (3)–(5)), to ob-  
558 tain  $r_{\text{EF}}^{1130}$  and consequently the EF diurnal course  $EF_{\text{Sim}}^{\text{ASTER}}$ .  
559 Instantaneous  $AE^{\text{ASTER}}$  is used in Eq. (7) to calculate half-  
560 hourly values of  $AE_{\text{Sim}}^{\text{ASTER}}$ . Finally, the ET diurnal course  
561  $ET_{\text{EF,Sim}}^{\text{ASTER}}$  is obtained from Eq. (6) using  $AE_{\text{Sim}}^{\text{ASTER}}$  and  $EF_{\text{Sim}}^{\text{ASTER}}$ .  
562 Fig. 10 displays the validation of  $ET_{\text{EF,Sim}}^{\text{ASTER}}$ . Linear regression  
563 yields  $ET_{\text{EF,Sim}}^{\text{ASTER}} = 0.77 ET_{\text{EC}} + 53$ , with  $R^2 = 0.63$  and  
564  $\text{RMSE} = 48 \text{ W m}^{-2}$ . These moderate performances can result  
565 from 1/amplifications through the ET calculation of errors  
566 on remotely sensed variables, 2/assuming daytime albedo  
567 is constant which can be far from the reality (Jacob and Oli-  
568 oso, 2005), or 3/the error in  $H$  and AE simulations translates

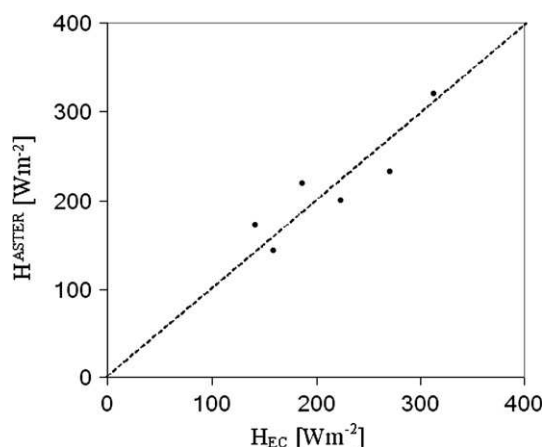


Figure 8a Comparison between sensible heat fluxes obtained from the eddy covariance system and sensible heat fluxes calculated using the model proposed by Lhomme et al. (1994) combined with ASTER thermal imagery.

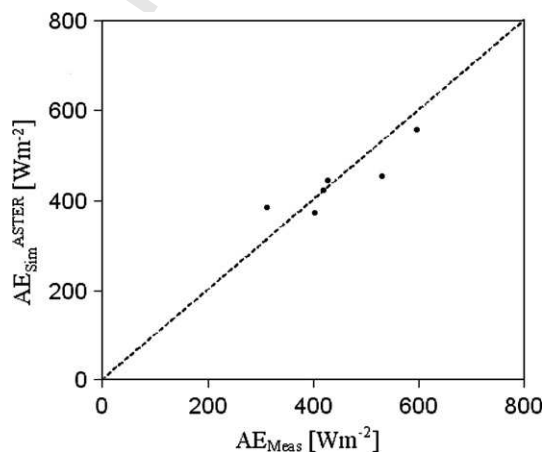


Figure 8b Comparison between measured available energy and that simulated using ASTER imagery.

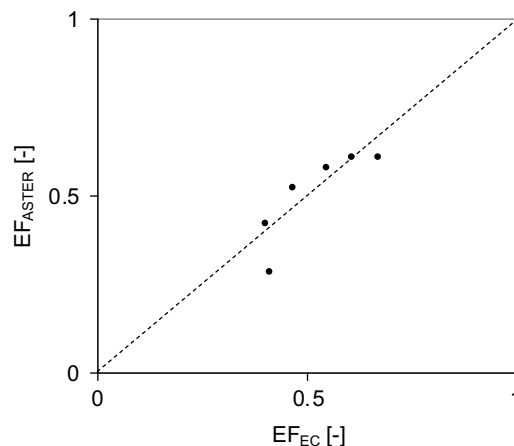
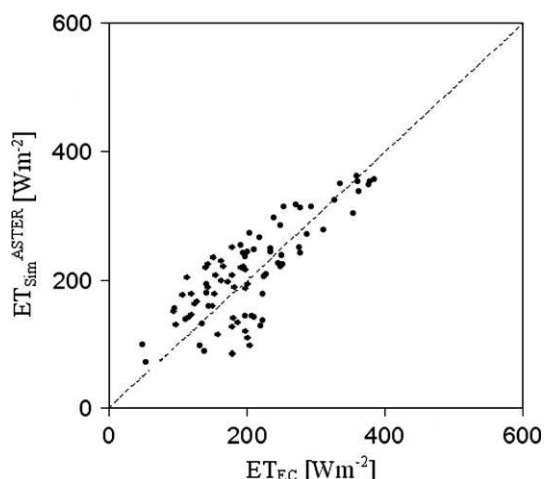


Figure 9 Eddy covariance derived evaporative fraction compared to ASTER derived evaporative fraction.



**Figure 10** Latent heat fluxes measured by the EC-system compared to latent heat fluxes calculated using both proposed formulations (for the evaporative fraction and for the available energy) with ASTER data.

569 directly into error in ET since it is estimated as the residual  
570 term of the energy balance equation, However, most ap-  
571 proaches devoted to estimating ET from remote sensing  
572 data are susceptible to comparable errors.

573 **Discussion and conclusion**

574 Sun synchronous optical remote sensing with high to moder-  
575 ate spatial resolution is often used for mapping instantane-  
576 ous sensible and latent heat fluxes and evaporative  
577 fraction EF. The latter is often assumed to be constant  
578 throughout the day, enabling the estimation of daily evapo-  
579 transpiration ET provided available energy AE is known. The  
580 daytime EF self preservation can be assumed under specific  
581 conditions, albeit sensitive to the time when EF is mea-  
582 sured. The current study shows although EF remains fairly  
583 constant during daytime under dry conditions, but it depicts  
584 a concave up shape under wet conditions. Since the latter  
585 correspond to large evaporative fluxes, using a constant  
586 EF value throughout the day induces large errors in the cal-  
587 culation of daily ET.

588 Parameterizing the EF diurnal course from remotely  
589 sensed instantaneous estimates is twofold, with the goal  
590 of well reproducing a concave up shape under wet condi-  
591 tions while EF is self preserved under dry conditions. The  
592 first step integrates incoming solar radiation and relative  
593 humidity, two main factors for atmospheric demand given  
594 air temperature is indirectly considered through relative  
595 humidity whereas the impact of wind speed is minor. By first  
596 including these two atmospheric factors in the formulation,  
597 the EF diurnal course is well reproduced. The second step of  
598 the parameterization consists of incorporating land surface  
599 condition, since soil moisture and vegetation control the EF  
600 absolute value and day-to-day variations. Thus, the day to  
601 day variation as well as the spatial heterogeneities is taken  
602 into account by correcting EF from remotely sensed instan-  
603 taneous ET.

604 This approach seems to include enough information on  
605 both atmospheric demand and land surface conditions to ac-

count for the diurnal and day-to-day fluctuations of EF – at  
at least – under the prevailing conditions over the study site.  
However, this parameterization does not include the ET regu-  
lation by stomatal conductance. Thus, the relationship  
developed here is not universal, it needs to be assessed  
for more diverse ecosystems since plants differently respond  
to water stress whereas stomatal regulation depends on soil  
moisture. One might indeed expect that for trees for in-  
stance the physiological control on stem water storage or  
release would significantly affect the diurnal course of EF.  
Either the physiological control in our olive yard is mild in  
potential conditions, or the empirical equation used to de-  
rive the diurnal shape of EF takes into account the net ef-  
fect of EF increase due to lower RH values and stomatal  
closure in the afternoon. Therefore, despite this empirical  
feature, the proposed approach is relevant for local applica-  
tions. Indeed, its implementation over the considered  
Moroccan olive orchard decreases errors on water consump-  
tion estimates from 8% to 1% in relative, as compared to  
assuming EF is self preserved.

The next step towards estimating daily ET is deriving the  
AE diurnal course from a practical relationship. As for EF, a  
heuristic approach is used, which relies on variables either  
available from remote sensing data or fairly constant over  
areas up to several kilometers. Thus, the AE diurnal course  
is derived from remotely sensed AE when TERRA/ASTER  
overpasses, to be used along with meteorological observa-  
tions for incoming shortwave and long wave irradiances.  
Though the proposed parameterization considers surface al-  
bedo is constant, the validation emphasizes good perfor-  
mances, with differences in AE lower than  $30 \text{ W m}^{-2}$ .

Once EF and AE are parameterized, the framework is ap-  
plied to ASTER data, using a simple energy balance model  
(Santanello and Friedl, 2003; Lhomme and Elguero, 1999).  
The methodology is next applied to derive the ET diurnal  
course. After analyzing the footprint configuration, valida-  
tion shows performances are comparable to other methods  
under similar conditions and data availabilities (Crow and  
Kustas, 2005). As for remote sensing approaches devoted  
to estimate daily ET, the proposed method is sensitive to er-  
rors on remotely sensed parameters. However, optimal use  
of in situ and remote sensing data allows a compromise be-  
tween loosing (respectively gaining) local (respectively re-  
gional) information. For operational applications, a  
temporal sampling of few days is needed. This is currently  
not possible with high spatial resolution TIR imagery, but  
could be in the near future. In the meanwhile, disaggrega-  
tion of low spatial resolution thermal remote sensing data  
can be a possible solution; however this issue is still subject  
of ongoing investigations. Finally, it is of interest to mention  
that this proposed method has been recently applied to a  
mosaic of agricultural fields in northern Mexico to very  
encouraging results (Chehbouni et al., 2007c).

**Acknowledgments**

This study has been funded by IRD, additional funding was  
provided by E.U. through the PLEIADES project. We are very  
grateful to all SUDMED research and technical staff for their  
help during the course of the experiment

664 **References**

- 665 Abrams, M., 2000. The advanced spaceborne thermal emission and  
666 reflection radiometer (ASTER): data products for the high spatial  
667 resolution imager on NASA's Terra platform. *International*  
668 *Journal of Remote Sensing* 21 (5), 847–859.
- 669 Abrams, M., Hook, S., 2002. ASTER User Handbook Jet Propulsion  
670 Laboratory. Pasadena, California, 135 pp.
- 671 Allen, R.G., 2000. Using the FAO-56 dual crop coefficient method  
672 over an irrigated region as part of an evapotranspiration  
673 intercomparison study. *Journal of Hydrology* 229, 27–41.
- 674 Allen, R.G., Tasumi, M., Trezza, R., 2007. Satellite-based energy  
675 balance for mapping evapotranspiration with internalized cali-  
676 bration (METRIC) – model. *Journal of Irrigation and Drainage*  
677 *Engineering* 133 (4), 380–394.
- 678 Asrar, G., Fuchs, M., Kanemasu, E.T., Hatfield, J.L., 1984.  
679 Estimating absorbed photosynthetic radiation and leaf area  
680 index from spectral reflectance in wheat. *Agronomy Journal* 76,  
681 300–306.
- 682 Baldocchi, D., 1997. Flux footprints within and over forest canopies.  
683 *Boundary-Layer Meteorology* 85, 273–292.
- 684 Baldocchi, D.D., Xu, L.K., Kiang, N., 2004. How plant functional-type,  
685 weather, seasonal drought, and soil physical properties alter  
686 water and energy fluxes of an oak-grass savanna and an annual  
687 grassland. *Agricultural and Forest Meteorology* 123, 13–39.
- 688 Bastiaanssen, W.G.M., Menenti, M., Feddes, R.A., Holtslag, A.A.,  
689 1998. A remote sensing surface energy balance algorithm for  
690 land (SEBAL): I. Formulation.. *Journal of Hydrology* 212–213 (1–  
691 4), 198–212.
- 692 Bastiaanssen, W.G.M., Molden, D.J., Makin, I.W., 2000. Remote  
693 sensing for irrigated agriculture: examples from research and  
694 possible applications. *Agricultural Water Management* 46, 137–  
695 155.
- 696 Batra, N., Islam, S., Venturini, V., Bisht, G., Jiang, L., 2006.  
697 Estimation and comparison of evapotranspiration from MODIS  
698 and AVHRR sensors for clear sky days over the Southern Great  
699 Plains. *Remote Sensing of Environment* 103, 1–15.
- 700 Bisht, G., Venturini, V., Jiang, L., Islam, S., 2005. Estimation of the  
701 net radiation using MODIS (moderate resolution imaging spect-  
702 roradiometer) data for clear sky days. *Remote Sensing of*  
703 *Environment* 97, 52–67.
- 704 Braud, I., Dantas Antonino, A.C., Vauclin, M., Thony, J.L., Ruelle,  
705 P.A., 1995. Simple Soil Plant Atmosphere Transfer model  
706 (SiSPAT) development and field verification. *Journal of Hydrol-  
707 ogy* 166, 213–250.
- 708 Brutsaert, W., 1982. *Evaporation into the Atmosphere*. Reidel,  
709 Dordrecht, 299 pp.
- 710 Calvet, J.-C., Noilhan, J., Roujean, J.-L., Bessemoulin, P., Cab-  
711 elguenne, M., Olioso, A., Wigneron, J.-P., 1998. An interactive  
712 vegetation SVAT model tested against data from six contrasting  
713 sites. *Agricultural and Forest Meteorology* 92, 73–95.
- 714 Caparrini, F., Castelli, F., Entekhabi, D., 2003. Mapping of land-  
715 atmosphere heat fluxes and surface parameters with remote  
716 sensing data. *Boundary-Layer Meteorology* 107, 605–633.
- 717 Caparrini, F., Castelli, F., Entekhabi, D., 2004. Variational estima-  
718 tion of soil and vegetation turbulent transfer and heat flux  
719 parameters from sequences of multisensor imagery. *Water*  
720 *Resources Research* 40, W12515. doi:10.1029/2004WR00335.
- 721 Chandrapala, L., Wimalasuriya, M., 2003. Satellite measurements  
722 supplemented with meteorological data to operationally estimate  
723 evaporation in Sri Lanka. *Agricultural Water Management*  
724 58, 89–107.
- 725 Chaponnière, A., Boulet, G., Chehbouni, A., Aresmouk, M., 2007.  
726 Understanding hydrological processes with scarce data in a  
727 mountain environment. *Hydrological Processes*. doi:10.1002/  
728 hyp.677.
- 729 Chehbouni, A., Escadafal, R., Boulet, G., Duchemin, B., Simonne-  
730 aux, V., Dedieu, G., Mougnot, B., Khabba, S., Kharrou, H.,  
731 Merlin, O., Chaponnière, A., Ezzahar, J., Er-Raki, S., Hoedjes,  
732 J., Hadria, R., Abourida, H., Cheggour, A., Raibi, F., Hanich, L.,  
733 Guemouria, N., Chehbouni, A., Olioso, A., Jacob, F. and  
734 Sobrino, J., in press-a. The Use of Remotely Sensed data for  
735 Integrated Hydrological Modeling in Arid and Semi-Arid  
736 Regions: the SUDMED Program. *International Journal of Remote*  
737 *Sensing*. Q2 737
- 738 Chehbouni, A., Ezzahar, J., Watts, C., Rodriguez, J.-C., Garatuza-  
739 Payan, J., in press-b. Estimating area-averaged surface fluxes  
740 over contrasted agricultural patchwork in a semi-arid region. In:  
741 Joachim Hill, Achim Röder (Eds.), *Advances in Remote Sensing*  
742 *and Geoinformation Processing for Land Degradation Assess-  
743 ment*, Taylor and Francis. 743
- 744 Chehbouni, A., Hoedjes, J., Rodriguez, J.-C., Watts, C., Garatuza,  
745 J., Jacob, F., Kerr, Y.H., 2007c. Using remotely sensed data to  
746 estimate area-averaged daily surface fluxes over a semi-arid  
747 mixed agricultural land. *Agricultural and Forest Meteorology*.  
748 doi:10.1111/j.1365-2486.2007.01466. 748
- 749 Choudhury, B.J., Monteith, J.L., 1988. A four-layer model for the  
750 heat budget of homogeneous land surfaces. *Quarterly Journal of*  
751 *the Royal Meteorological Society* 114, 373–398. 751
- 752 Cleugh, H.A., Leuning, R., Mu, Q., Running, S.W., 2007. Regional  
753 evaporation estimates from flux tower and MODIS satellite data.  
754 *Remote Sensing of Environment* 106, 285–304. 754
- 755 Coudert, B., Ottlé, C., Boudevillain, B., Demarty, J., Guillevic, P.,  
756 2006. Contribution of Thermal Infrared remote sensing data in  
757 multiobjective calibration of a dual source SVAT model. *Journal*  
758 *of Hydrometeorology* 7 (3), 404–420. 758
- 759 Crago, R.D., 1996. Conservation and variability of the evaporative  
760 fraction during daytime. *Journal of Hydrology* 180, 173–194. 760
- 761 Crago, R.D., Brutsaert, W., 1996. Daytime evaporation and the self-  
762 preservation of the evaporative fraction and the Bowen ratio.  
763 *Journal of Hydrology* 178, 241–255. 763
- 764 Crow, W.T., Kustas, W.P., 2005. Utility of assimilating surface  
765 radiometric temperature observations for evaporative fraction  
766 and heat transfer coefficient retrieval. *Boundary-Layer Meteoro-*  
767 *logy* 115, 105–130. 767
- 768 Duchemin, B., Hadria, R., Er-Raki, S., Boulet, G., Maisongrande, P.,  
769 Chehbouni, A., Escadafal, R., Ezzahar, J., Hoedjes, J., Kharrou,  
770 M.H., Khabba, S., Mougnot, B., Olioso, A., Rodriguez, J.-C.,  
771 Simonneaux, V., 2006. Monitoring wheat phenology and irriga-  
772 tion in Center of Morocco: on the use of relationship between  
773 evapotranspiration, crops coefficients, leaf area index and  
774 remotely-sensed vegetation indices. *Agricultural Water Manage-*  
775 *ment* 79, 1–27. 775
- 776 Er-Raki, S., Chehbouni, A., Guemouria, N., Duchemin, B., Ezzahar,  
777 J., Hadria, R., 2007a. Combining FAO-56 model and ground-  
778 based remote sensing to estimate water consumptions of wheat  
779 crops in a semi-arid region. *Agricultural water management* 87,  
780 41–54. 780
- 781 Er-Raki, S., Chehbouni, A., Hoedjes, J., Ezzahar, J., Duchemin, B.,  
782 Jacob, F., 2007b. Assimilation of ASTER based ET estimates in  
783 FAO 56 model over olive orchards in a semi-arid region.  
784 *Agricultural water management*. doi:10.1016/j.agwat.2007.  
785 10.01. 785
- 786 Finn, D., Lamb, B., Leclerc, M.Y., Horst, T.W., 1996. Experimental  
787 evaluation of analytical and Lagrangian surface-layer footprint  
788 models. *Boundary-Layer Meteorology* 80, 283–308. 788
- 789 French, A.N., Jacob, F., Anderson, M.C., Kustas, W.P., Timmer-  
790 mans, W., Gieske, A., Su, B., Su, H., McCabe, M.F., Li, F.,  
791 Prueger, J., Brunsell, N., 2005. Surface energy fluxes with the  
792 Advanced Spaceborne Thermal Emission and Reflection radiom-  
793 eter (ASTER) at the Iowa 2002 SMACEX site (USA). *Remote*  
794 *Sensing of Environment* 99, 55–65. 794
- 795 Fujisada, H., 1998. ASTER Level-1 data processing algorithm. *IEEE*  
796 *Transactions on Geoscience and Remote Sensing* 36, 1101–1112.  
797 796
- 797 Fujisada, H., Sakuma, F., Ono, A., Kudoh, M., 1998. Design and  
798 preflight performance of ASTER instrument protoflight model. 798

- 799 IEEE Transactions on Geoscience and Remote Sensing 36 (4),  
800 1152–1160.
- 801 Gentine, P., Entekhabi, D., Chehbouni, A., Boulet, G., Duchemin,  
802 B., 2007. Analysis of evaporative fraction diurnal behaviour.  
803 *Agricultural and Forest Meteorology* 143, 13–29.
- 804 Gillespie, A., Rokugawa, S., Matsunaga, T., Cothorn, J.S., Hook,  
805 S.J., Kahle, A.B., 1998. A temperature and emissivity separation  
806 algorithm for Advanced Spaceborne Thermal Emission and  
807 Reflection Radiometer (ASTER) images. *IEEE Transactions on*  
808 *Geoscience and Remote Sensing* 36 (4), 1113–1126.
- 809 Glenn, E.P., Huete, A.R., Nagler, P.L., Hirschboeck, K.K., Brown,  
810 P., 2007. Integrating remote sensing and ground methods to  
811 estimate evapotranspiration. *Critical Reviews in Plant Sciences*  
812 26 (3), 139–168.
- 813 Gomez, M., Sobrino, J., Oliso, A., Jacob, F., 2005. Retrieval of  
814 evapotranspiration over the Alpillles test site using PolDER and  
815 thermal camera data. *Remote Sensing of Environment* 96, 399–  
816 408.
- 817 Hoedjes, J.C.B., Zuurbier, R.M., Watts, C.J., 2002. Large aperture  
818 scintillometer used over a homogeneous irrigated area, partly  
819 affected by regional advection. *Boundary-Layer Meteorology*  
820 105, 99–117.
- 821 Hoedjes, J.C.B., Chehbouni, A., Ezzahar, J., Escadafal, R., De  
822 Bruin, H.A.R., 2007. Comparison of large aperture scintillometer  
823 and Eddy covariance measurements: can thermal infrared data  
824 be used to capture footprint induced differences? *Journal of*  
825 *Hydrometeorology* 8, 144–159.
- 826 Horst, T.W., Weil, J.C., 1992. Footprint estimation for scalar flux  
827 measurements in the atmospheric surface layer. *Boundary-Layer*  
828 *Meteorology* 59, 279–296.
- 829 Horst, T.W., Weil, J.C., 1994. How far is far enough?: The fetch  
830 requirements for micrometeorological measurement of surface  
831 fluxes. *Journal of Oceanic and Atmospheric Technology* 11,  
832 1018–1025.
- 833 Jackson, R.D., Reginato, R.J., Idso, S.B., 1977. Wheat canopy  
834 temperature: a practical tool for evaluating water require-  
835 ments. *Water Resources Research* 13, 651–656.
- 836 Jackson, R.D., Hatfield, J.L., Reginato, R.J., Idso, S.B., Pinter Jr.,  
837 P.J., 1983. Estimation of daily evapotranspiration from one  
838 time-of-day measurements. *Agricultural Water Management* 7,  
839 351–362.
- 840 Jacob, F., Weiss, M., Oliso, A., French, A., 2002. Assessing the  
841 narrowband to broadband conversion to estimate visible, near  
842 infrared and shortwave apparent albedo from airborne PolDER  
843 data. *Agronomie: Agriculture and Environment* 22, 537–546.
- 844 Jacob, F., Petitcolin, F., Schmugge, T., Vermote, E., French, A.,  
845 Ogawa, K., 2004. Comparison of land surface emissivity and  
846 radiometric temperature derived from MODIS and ASTER sen-  
847 sors. *Remote Sensing of Environment* 90, 137–152.
- 848 Jacob, F., Oliso, A., 2005. Derivation of diurnal courses of albedo  
849 and reflected solar irradiance from airborne POLDER data  
850 acquired near solar noon. *Journal of Geophysical Research*  
851 110, D10104. doi:10.1029/2004JD00488.
- 852 Jacob, F., Schmugge, T., Oliso, A., French, A., Courault, D.,  
853 Ogawa, K., Petitcolin, F., Chehbouni, G., Pinheiro, A., Privette,  
854 J., in press. Modeling and inversion in thermal infrared remote  
855 sensing over vegetated land surfaces. In: *Advances in Land*  
856 *Remote Sensing: System, Modeling, Inversion and Application* (S.  
857 Q5 Liang Ed.), Springer.
- 858 Leclerc, M.Y., Shen, S., Lamb, B., 1997. Observations and large-  
859 Eddy simulation modeling of footprints in the lower convective  
860 boundary layer. *Journal of Geophysical Research* 102, 9323–  
861 9334.
- 862 Lhomme, J.-P., Monteny, B., Amadou, M., 1994. Estimating sensible  
863 heat flux from radiometric temperature over sparse millet.  
864 *Agricultural and Forest Meteorology* 68, 77–91.
- 865 Lhomme, J.-P., Elguero, E., 1999. Examination of evaporative  
866 fraction diurnal behaviour using a soil-vegetation model coupled  
with a mixed-layer model. *Hydrology and Earth System Sciences*  
3 (2), 259–270.
- Li, S.-G., Eugster, W., Asanuma, J., Kotani, A., Davaa, G.,  
Oyunbaatar, D., Sugita, M., 2006. Energy partitioning and its  
biophysical controls above a grazing steppe in central  
Mongolia. *Agricultural and Forest Meteorology* 137 (1–2),  
89–106.
- Liu, Y., Hiyama, T., Yamaguchi, Y., 2006. Scaling of land surface  
temperature using satellite data: a case examination on ASTER  
and MODIS products over a heterogeneous terrain area. *Remote*  
*Sensing of Environment* 105, 115–128.
- Mahfouf, J.F., Manzi, A.O., Noilhan, J., Giordani, H., Déqué, M.,  
1995. The land surface scheme ISBA within the Météo-France  
climate model ARPEGE. Part I. Implementation and preliminary  
results. *Journal of Climate* 8, 2039–2057.
- Mu, Q., Heinsch, F.A., Zhao, M., Running, S.W., 2007. Development  
of a global evapotranspiration algorithm based on MODIS and  
global meteorology data. *Remote Sensing of Environment* 111  
(4), 519–536.
- Nichols, W.E., Cuenca, R.H., 1993. Evaluation of the evaporative  
fraction for parameterization of the surface, energy-balance.  
*Water Resources Research* 29, 3681–3690.
- Norman, J.M., Anderson, M.C., Kustas, W.P., French, A.N., Meci-  
kalski, J., Torn, R., Diak, G.R., Schmugge, T.J., Tanner, B.C.W.,  
2003. Remote sensing of surface energy fluxes at 10<sup>1</sup>-m pixel  
resolutions. *Water Resources Research* 39 (8), 1221.  
doi:10.1029/2002WR00177.
- Ogawa, K., Schmugge, T., Jacob, F., French, A., 2003. Estimation  
of land surface window (8–12 μm) emissivity from multi-spectral  
thermal infrared remote sensing—A case study in a part of Sahara  
Desert. *Geophysical Research Letters* 30, 1067–1071.
- Ohmura, A., Wild, M., 2002. Is the hydrological cycle accelerating?  
*Science* 298, 1345–1346.
- Oliso, A., Carlson, T.N., Brisson, N., 1996. Simulation of diurnal  
transpiration and photo-synthesis of a water stressed soybean  
crop. *Agricultural and Forest Meteorology* 81, 41–59.
- Oliso, A., Inoue, Y., Ortega-Farias, S., Demarty, J., Wigneron, J.-  
P., Braud, I., Jacob, F., Lecharpentier, P., Otlé, C., Calvet, J.-  
C., Brisson, N., 2005. Future directions for advanced evapo-  
transpiration modeling: assimilation of remote sensing data into  
crop simulation models and SVAT models. *Irrigation and Drain-  
age Systems* 19 (3–4), 355–376.
- Porporato, A., Daly, E., Rodriguez-Iturbe, I., 2004. Soil water  
balance and ecosystem response to climate change. *American*  
*Naturalist* 164, 625–632.
- Rannik, Ü., Aubinet, M., Kurbanmuradov, O., Sabelfeld, K.K.,  
Markkanen, T., Vesala, T., 2000. Footprint analysis for mea-  
surements over a heterogeneous forest. *Boundary-Layer Mete-  
orology* 97, 137–166.
- Roerink, G.J., Su, Z., Menenti, M., 2000. S-SEBI: a simple remote  
sensing algorithm to estimate the surface energy balance.  
*Physics and Chemistry of the Earth (B)* 25 (2), 147–157.
- Santanello, J.A., Friedl, M.A., 2003. Diurnal covariation in soil heat  
flux and net radiation. *Journal of Applied Meteorology* 42, 851–  
862.
- Schmugge, T., Hook, S.J., Coll, C., 1998. Recovering surface  
temperature and emissivity from thermal infrared multispectral  
data. *Remote Sensing of Environment* 65 (2), 121–131.
- Schuepp, P.H., Leclerc, M.Y., MacPherson, J.I., Desjardins, R.L.,  
1990. Footprint prediction of scalar fluxes from analytical  
solutions of the diffusion equation. *Boundary-Layer Meteorology*  
50, 355–373.
- Schuurmans, J.M., Troch, P.A., Veldhuizen, A.A., Bastiaanssen,  
W.G.M., Bierkens, M.F.P., 2003. Assimilation of remotely sensed  
latent heat flux in a distributed hydrological model. *Advances in*  
*Water Resources* 26, 151–159.
- Seguin, B., Assad, E., Freteaud, P., Imbernon, J.-P., Kerr, Y.H.,  
Lagouarde, J.-P., 1989. Use of meteorological satellites for

- 935 water balance monitoring in Sahelian regions. *International*  
936 *Journal of Remote Sensing* 10, 1001–1017.
- 937 Shuttleworth, W.J., Gurney, R.J., Hsu, A.Y., Ormsby, J.P.,  
938 1989FIFE: The Variation in Energy Partition at Surface Flux  
939 Sites, vol. 186. IAHS Publication, pp. 67–74.
- 940 Shuttleworth, W.J., Gurney, R.J., 1990. The theoretical relation-  
941 ship between foliage temperature and canopy resistance in  
942 sparse crops. *Quarterly Journal of the Royal Meteorological*  
943 *Society* 116, 497–519.
- 944 Sugita, M., Brutsaert, W., 1991. Daily evaporation over a region  
945 from lower boundary layer profiles. *Water Resources Research*  
946 27, 747–752.
- 947 Suleiman, A., Crago, R.D., 2004. Hourly and daytime evapotrans-  
948 piration from grassland using radiometric surface temperatures.  
949 *Agronomy Journal* 96, 384–390.
- 950 Twine, T.E., Kustas, W.P., Norman, J.M., Cook, D.R., Houser, P.R.,  
951 Meyers, T.P., Prueger, J.H., Starks, P.J., Wesely, M.L., 2000.  
952 Correcting Eddy-covariance flux underestimates over a grass-  
953 land. *Agricultural and Forest Meteorology* 103, 279–300.
- 954 Thome, K., Palluconi, F., Takashima, T., Masuda, K., 1998.  
955 Atmospheric correction of ASTER. *IEEE Transactions on Geosci-*  
956 *ence and Remote Sensing* 36, 1199–1211.
- 957 Van den Hurk, B.J.J.M., Bastiaanssen, W.G.M., Pelgrum, H., Van  
958 Meijgaard, E., 1997. A new methodology for initialization of soil  
959 moisture fields in numerical weather prediction models using  
960 METEOSAT and NOAA data. *Journal of Applied Meteorology* 36,  
961 1271–1283.
- 962 Van Dijk, A., Moene, A.F. De Bruin, H.A.R., 2004. The principles of  
963 surface flux physics: theory, practice and description of the  
964 ECPACK library. Internal Report 2004/1, Meteorology and Air  
Quality Group, Wageningen University, Wageningen, The Neth-  
erlands, 99 pp.
- 965  
966  
967 Wang, K., Li, Z., Cribb, M., 2006. Estimation of evaporative  
968 fraction from a combination of day and night land surface  
969 temperatures and NDVI: a new method to determine the  
970 Priestley-Taylor parameter. *Remote Sensing of Environment*  
971 102, 293–305.
- 972 Weiss, M., Jacob, F., Baret, F., Pragnère, A., Bruchou, C., Leroy,  
973 M., Hautecoeur, O., Prévot, L., Bruguier, N., 2002. Evaluation  
974 of kernel-driven BRDF models for the normalization of Alpilles/  
975 ReSeDA POLDER data. *Agronomy* 22, 531–536.
- 976 Wild, M., Ohmura, A., Gilgen, H., Rosenfeld, D., 2004. On the  
977 consistency of trends in radiation and temperature records and  
978 implications for the global hydrological cycle. *Geophysical*  
979 *Research Letters* 31, L11201. doi:10.1029/2003GL01918.
- 980 Williams, D.G., Cable, W., Hultine, K., Hoedjes, J.C.B., Yopez,  
981 E.A., Simonneaux, V., Er-Raki, S., Boulet, G., De Bruin, H.A.R.,  
982 Chehbouni, A., Hartogensis, O.K., Timouk, F., 2004. Evapo-  
983 transpiration components determined by stable isotope, sap  
984 flow and eddy covariance techniques. *Agricultural and Forest*  
985 *Meteorology* 125, 241–258.
- 986 Yang, F., White, M.A., Michaelis, A.R., Ichii, K., Hashimoto, H.,  
987 Votava, P., Zhu, A-X., Nemani, R.R., 2006. Prediction of  
988 continental-scale evapotranspiration by combining MODIS and  
989 AmeriFlux data through support vector machine. *IEEE Trans-*  
990 *actions on Geoscience and Remote Sensing* 44 (11), 3452–  
991 3461.
- 992 Zhang, L., Lemeur, R., 1995. Evaluation of daily evapotranspiration  
993 estimates from instantaneous measurements. *Agricultural and*  
994 *Forest Meteorology* 74, 139–154.
- 995